Available online at www.sciencedirect.com
SCIENCE DIRECT®
Journal of Power Sources 132 (2004) 64–70
JOURNAL OF POWER SOURCES
www.elsevier.com/locate/jpowsour

Prediction of production power for high-pressure hydrogen by high-pressure water electrolysis

Kazuo Onda*, Takahiro Kyakuno, Kikuo Hattori, Kohei Ito

Toyohashi University of Technology, 1-1 Hibarigaoka, Tenpaku, Toyohashi, Aichi 441-8580, Japan

Received 6 August 2003; received in revised form 15 October 2003; accepted 24 January 2004

Abstract

Recent attention focused on fuel cell electric vehicles (FCEVs) has created demand for the construction of hydrogen supply stations for FCEVs throughout the world. The hydrogen pressure supplied at the supply stations is intentionally high to increase the FCEVs driving mileage. Water electrolysis can produce clean hydrogen by utilizing electricity from renewable energy without CO_2 emission to the atmosphere when compared with the industrial fossil fuel reforming process. The power required for high-pressure water electrolysis, wherein water is pumped up to a high-pressure, may be less than the power required for atmospheric water electrolysis, wherein the produced atmospheric hydrogen is pumped by a compressor, since the compression power for water is much less than that for hydrogen-gas. In this study, the ideal water electrolysis voltage of up to 70 MPa and 250 °C is estimated by referring to both the results of LeRoy et al. up to 10 MPa and 250 °C, and the latest steam tables. Using this high-pressure water electrolysis voltage, the power required to produce high-pressure hydrogen by high-pressure water electrolysis is estimated to be about 5% less than that required for atmospheric water electrolysis, assuming compressor and pump efficiencies of 50%.

Keywords: Water electrolysis; Hydrogen production; High-pressure hydrogen; Water electrolysis voltage

1. Introduction

In recent years, the attention focused on high-efficiency and low-polluting fuel cell vehicles has increased demand for hydrogen as a vehicle fuel. Many countries are investigating the compression of hydrogen up to 700 atm (1 atm = 0.101325 MPa) to increase the volume of on-board hydrogen at experimental hydrogen supplying stations. There are various methods of manufacturing hydrogen, including fossil fuel reforming, saltwater electrolysis, and water electrolysis. The present study focuses on water electrolysis for manufacturing hydrogen from water without the use of fossil fuels. Recently, water electrolysis performance has improved through the use of polymer electrolyte membranes, which have improved energy efficiency beyond conventional alkali water electrolysis [1]. In polymer electrolyte water electrolysis at atmospheric pressure, water electrolysis cell characteristics, such as current and temperature distributions in the cell, are being investigated experimentally and analytically in regard to the effects of overvoltage and saturated water vapor [2]. High-pressure water electrolysis up to 100 atm has been studied by LeRoy et al. [3], who give equations for electrolysis voltage of KOH aqueous solution considering an effect of saturated water vapor pressure.

Since less power is generally required to compress liquid water than to compress gaseous hydrogen, it is reasonable to conclude that the preparation of high-pressure hydrogen by electrolysis of previously prepared high-pressure water would require less power than using a compressor to compress gaseous hydrogen obtained through water electrolysis at atmospheric pressure. In referring to the water electrolysis voltage equations presented by LeRoy et al., we have calculated the ideal energy for water electrolysis from 1 to 700 atm without regard to the effects of overvoltage or saturated water vapor, and prepared basic data for showing the effectiveness of high-pressure water electrolysis. Although LeRoy et al. have considered the latent heat of water vapor saturating the generated hydrogen and oxygen in their calculation of the electrolysis voltage, the influence of saturated water vapor at high-pressure is negligible because the effect of saturated water vapor decreases in inverse proportion to the operating high-pressure of water electrolysis. Furthermore, since the overvoltage is reduced

* Corresponding author. Tel.: +81-532-44-6722; fax: +81-532-44-6722.
E-mail address: onda@eee.tut.ac.jp (K. Onda).

0378-7753/$ – see front matter © 2004 Elsevier B.V. All rights reserved.
doi:10.1016/j.jpowsour.2004.01.046

Nomenclature

a–e	specific heat coefficient
B	virial constant (cm^3/mol)
C	virial constant (cm^6/mol^2)
$E_{t,p}$	water electrolysis voltage (V) at t (°C) and p (atm)
g	gravitational acceleration (m/s^2)
G	Gibbs energy (J/mol)
h	water head (m)
H	enthalpy (J/mol)
Q_N	intake-gas volume flow rate ($N\,m^3/h$)
S	entropy (J/(mol K))
$V_{t,p}$	enthalpy voltage (V) at t (°C) and p (atm)
W	power (W)
z	compressibility factor
$-\Delta G$	Gibbs energy of water formation (J/mol)
$-\Delta G^{\circ}_{H_2O}$	Gibbs energy of water formation under the standard condition (J/mol)
$-\Delta H$	enthalpy of water formation (J/mol)
$-\Delta H^{\circ}_{H_2O}$	enthalpy of water formation under the standard condition (J/mol)
$-\Delta S$	entropy of water formation (J/(mol K))
$-\Delta S^{\circ}_{H_2O}$	entropy of water formation under the standard condition (J/(mol K))

Greek letters

κ	ratio of specific heat
ρ	water density (kg/m^3)

Subscripts and superscripts

comp	compressor
ele	water electrolysis
H_2	hydrogen
H_2O	water
O_2	oxygen
p	pressure
pump	water pump
t	temperature

similarly to fuel cells when the operating pressure of solid polymer water electrolysis is increased, this aspect is also beneficial [4]. In this report, the power needed to compress hydrogen produced by atmospheric water electrolysis to 700 atm, and the power required to operate a high-pressure water pump for high-pressure water electrolysis are calculated, and then the power requirements for low-pressure water electrolysis and high-pressure water electrolysis are compared. However, only the ideal power to electrolyze water without any overpotential loss is used to estimate the production power of high-pressure hydrogen, because it is difficult to estimate realistic electrolyzing power due to the lack of experimental data for high-pressure water electrolysis.

2. Basic equations of energy for water electrolysis

2.1. Basic equations of energy

Energy is produced when stoichiometric amounts of gaseous hydrogen and oxygen react with each other to produce liquid water, as shown in Eq. (1). In the case of polymer electrolyte membrane fuel cells, electrochemical reaction as shown in Eq. (2) proceeds at the hydrogen electrode, and reaction as shown in Eq. (3) proceeds at the oxygen electrode. In Eq. (2), two electrons are required for one hydrogen molecule

$$H_2 + \tfrac{1}{2}O_2 \rightarrow H_2O \quad (1)$$

$$H_2 \rightarrow 2H^+ + 2e^- \quad (2)$$

$$2H^+ + 2e^- + \tfrac{1}{2}O_2 \rightarrow H_2O \quad (3)$$

The exothermic heat generated by Eq. (1) is called the enthalpy of formation $-\Delta H$, which is described by other thermodynamic quantities as shown in Eq. (4). The Gibbs energy $-\Delta G$ in Eq. (4) can be converted to electrical energy while the entropy heat $-T\,\Delta S$ is released as heat. In Eq. (4), T and t represent temperature in K and °C, respectively, and p represents pressure in atm

$$-\Delta H(t, p) = -\Delta G(t, p) - T\,\Delta S(t, p) \quad (4)$$

Fig. 1 shows the energy Eq. (4) for the reaction of $H_2 + 0.5O_2 \leftrightarrow H_2O$ as the actual voltage and current (V–I) characteristics for both fuel cell and water electrolysis. The region on the right side of the figure represents a fuel cell, and the region on the left side represents water electrolysis. When hydrogen and oxygen react with each other ideally in a fuel cell, $-\Delta G$ becomes electricity and $-T\,\Delta S$ becomes heat. Conversely, when water is electrolyzed to produce hydrogen and oxygen by applying electricity, the electrical energy of $-\Delta G$ and the heat of $-T\,\Delta S$ are required. The enthalpy voltage $V_{t,p}$ is defined by Eq. (5), and the water electrolysis voltage $E_{t,p}$ is defined by Eq. (6)

$$V_{t,p} = \frac{-\Delta H(t, p)}{nF} \quad (5)$$

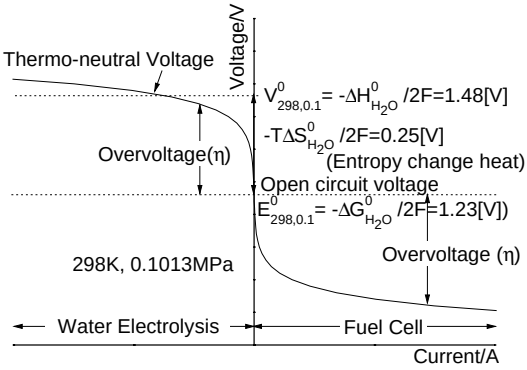

Fig. 1. Voltage–current characteristics for water electrolysis and fuel cell.

$$E_{t,p} = \frac{-\Delta G(t,\, p)}{nF} \tag{6}$$

where F represents the Faraday constant (96,485 (C/mol)), and n represents the number of electrons ($n = 2$ according to Eqs. (2) and (3) for water electrolysis) participating in the reaction. Since $V_{25,1}$ is equal to 1.48 V, and $E_{25,1}$ is equal to 1.23 V at the standard condition t_0, p_0 (25 °C, 1 atm) as shown in Fig. 1, $-T\,\Delta S/(2F) = 0.25$ V energy is supplied as heat [5]. In Fig. 1, the standard enthalpy of formation $-\Delta H^{\circ}_{H_2O}$ and the standard Gibbs energy of formation $-\Delta G^{\circ}_{H_2O}$ represent the enthalpy of formation and the Gibbs energy of formation under the standard condition, respectively.

The discussion above pertains to an ideal case without any loss, but in practice, losses by reaction, diffusion and resistance are inevitable, i.e. so-called overvoltage η is produced to form the realistic V–I curve shown in Fig. 1. η increases in conjunction with an increase in electrical current. When $2F\eta = -T\,\Delta S$ during electrolysis, external heat does not need to be supplied because the electrical energy participates in both $-\Delta G$ and $-T\,\Delta S$. This point ($V_{t,p} = -\Delta G/2F - T\,\Delta S/2F$) is called the thermo-neutral voltage, and is also equal to $-\Delta H/2F$. In this report, referring to the equations presented by LeRoy et al., we determine the change in pressure and temperature of the water electrolysis voltage $E_{t,p}$ and enthalpy voltage $V_{t,p}$ as shown below to discover the ideal electrolysis power under high-pressure disregarding the overvoltage caused by various losses.

The enthalpy of water formation $-\Delta H(t,\, 1)$ and Gibbs energy of water formation $-\Delta G(t,\, 1)$ at 1 (atm) and t (°C) can be expressed by Eqs. (7) and (8) below [5]

$$\Delta H(t,\, 1) = H_{H_2O}(t,\, 1) - H_{H_2}(t,\, 1) - \tfrac{1}{2} H_{O_2}(t,\, 1) \tag{7}$$

$$\Delta G(t,\, 1) = G_{H_2O}(t,\, 1) - G_{H_2}(t,\, 1) - \tfrac{1}{2} G_{O_2}(t,\, 1) \tag{8}$$

where $H_i(t,\, 1)$ and $G_i(t,\, 1)$ represent the enthalpy and Gibbs energy of chemical species i at t (°C) and 1 (atm), respectively, and can be described by the specific heat of chemical species i (H_2, O_2, H_2O) as shown later.

The enthalpy of water formation $-\Delta H(t,\, p)$ and Gibbs energy of water formation $-\Delta G(t,\, p)$ at t (°C) and p (atm) can be represented by Eqs. (9) and (10)

$$\Delta H(t,\, p) = H_{H_2O}(t,\, p) - H_{H_2}(t,\, p) - \tfrac{1}{2} H_{O_2}(t,\, p) \tag{9}$$

$$\Delta G(t,\, p) = G_{H_2O}(t,\, p) - G_{H_2}(t,\, p) - \tfrac{1}{2} G_{O_2}(t,\, p) \tag{10}$$

where $H_i(t, p)$ and $G_i(t, p)$ can be determined using the steam table and virial constant in the state equation of hydrogen and oxygen described later [3].

2.2. Temperature change of ΔH and ΔG [5]

ΔH and ΔG change depending on the temperature, and are calculated using the specific heat of hydrogen, oxygen and water. The temperature change of enthalpy $H_i(t,\, 1)$ and entropy $S_i(t,\, 1)$ of chemical species i are represented by Eqs. (11) and (12), where H_i° is designated as $H^{\circ}_{H_2} = H^{\circ}_{O_2} = 0$ and $H^{\circ}_{H_2O} = -\Delta H^{\circ}_{H_2O}$, and S_i° is the standard entropy of chemical species i, according to JANAF

$$\begin{aligned} H_i(t,\, 1) - H_i^{\circ} = {} & a(T - T_0) + \frac{b}{2} \times 10^{-3}(T^2 - T_0^2) \\ & - c \times 10^5 \left(\frac{1}{T} - \frac{1}{T_0} \right) \\ & - \frac{e}{2} \times 10^8 \left(\frac{1}{T^2} - \frac{1}{T_0^2} \right) \end{aligned} \tag{11}$$

$$\begin{aligned} S_i(t,\, 1) - S_i^{\circ} = {} & a(\ln T - \ln T_0) + b \times 10^{-3}(T - T_0) \\ & - \frac{c}{2} \times 10^5 \left(\frac{1}{T^2} - \frac{1}{T_0^2} \right) \\ & - \frac{e}{3} \times 10^8 \left(\frac{1}{T^3} - \frac{1}{T_0^3} \right) \end{aligned} \tag{12}$$

Items a through e in the above equations are specific heat coefficients, which are values from the Electrochemistry Handbook [5], and are shown in Table 1. Since the adaptable range of specific heat coefficients for water in Table 1 is 25–100 °C, data from the steam tables [6] were used for calculations above 100 °C, as described later. The consistency between the Electrochemistry Handbook and the steam tables was adequate for water up to 100 °C. $H_i(T)$ calculated by Eq. (11) was substituted in Eq. (7) to get the temperature change of $\Delta H(t,\, 1)$. The temperature change of $\Delta G(t,\, 1)$ was calculated by Eqs. (4), (11) and (12).

Table 1
Coefficients for specific heat

	a	b	c	e
H_2O (liquid)	72.39	9.38	–	–
H_2 (gas)	26.57	3.77	1.17	–
O_2 (gas)	34.35	1.92	−18.45	4.06

LeRoy et al. show the controlling equations of $E_{t,1}$ and $V_{t,1}$ for temperature change as the following Eqs. (13) and (14)

$$V_{t,1} = 1.4850 - 1.490 \times 10^{-4} t - 9.84 \times 10^{-8} t^2 \text{ (V)} \tag{13}$$

$$\begin{aligned} E_{t,1} = {} & 1.5184 - 1.5421 \times 10^{-3} T - 9.523 \times 10^{-5} T \ln T \\ & + 9.84 \times 10^{-8} T^2 \text{ (V)} \end{aligned} \tag{14}$$

The compatibility of Eqs. (7) and (13), and the compatibility of Eqs. (8) and (14) were adequate as described later.

2.3. Pressure change of ΔH and ΔG [3]

Since the pressure effects are not described in the Electrochemistry Handbook, we follow the controlling equation presented by LeRoy et al. When the state equations of hydrogen and oxygen use the virial constants B and C, the

Table 2
Coefficients of virial constant

	b_1	b_2	c_1	c_2
H_2	20.5	−1,857	−351	12,760
O_2	42.6	−17,400	−2604	61,457

enthalpy and Gibbs energy of hydrogen and oxygen can be expressed as shown in Eqs. (15) and (16)

$$H(t, p) - H(t, 1) = \left(B - T\frac{\partial B}{\partial T}\right)p + \frac{C - B^2 - (1/2)T((\partial C/\partial T) - 2B(\partial B/\partial T))}{RT}p^2 \quad (15)$$

$$G(t, p) - G(t, 1) = RT\ln p + Bp + \frac{C - B^2}{2RT}p^2 \quad (16)$$

where R is the gas constant (atm cm^3/(mol K)), and p is pressure (atm). Since the units of $H(t, p)$ and $G(t, p)$ in Eqs. (15) and (16) are (atm cm^3/mol), 1 (atm cm^3/mol) can be converted to 0.101325 (J/mol). The virial constants B and C are approximated in the following equations as functions of temperature

$$B = b_1 + \frac{b_2}{T}\ (\mathrm{cm}^3/\mathrm{mol}) \quad (17)$$

$$C = c_1 + \frac{c_2}{T^{1/2}}\ (\mathrm{cm}^6/\mathrm{mol}^2) \quad (18)$$

The values of coefficients b_1, b_2, c_1, and c_2 used in the above equation are shown in Table 2 for oxygen and hydrogen. The pressure range for LeRoy et al. is 1–100 atm, but since the data for up to 1000 atm are included in the managed virial constant, Eqs. (17) and (18) are assumed applicable in the present study up to 700 atm. Since the steam tables covers a wide range of pressure changes in $H(t, p)$ and $S(t, p)$ for water, these values were used in this study.

With regard to water production reaction in fuel cells, ΔH, ΔG, and ΔS have been described as negative in accordance with convention. However, in the present study as described below, the values of ΔH, ΔG, and ΔS are described as positive, avoiding complexity, to predict the hydrogen manufacturing power by water electrolysis.

3. Numerical results of temperature and pressure change of ΔH and ΔG

3.1. Standard enthalpy $\Delta H^\circ_{H_2O}$ and standard Gibbs energy $\Delta G^\circ_{H_2O}$ of formation

At first the $\Delta H^\circ_{H_2O}$ and $\Delta G^\circ_{H_2O}$ used by LeRoy et al. are compared with the those by the Electrochemistry Handbook [5] and by JANAF [7], as shown in Table 3. These values are shown in Table 4 as voltages. In Table 3, there are differences in the fourth and fifth decimal places. However, in the voltage table of Table 4, the values round off to four decimal places and match up to the fourth place. Since values are expressed at 1 bar (10^5 Pa) in JANAF, these values were revised at 1 atm in Table 4 by Eq. (19) [5]

$$\Delta G\ (10^5\ \mathrm{Pa}, T) = \Delta G\ (1\ \mathrm{atm}, T) - 0.1094T\ (\mathrm{J/mol}) \quad (19)$$

Table 3
Enthalpy and Gibbs energy for water electrolysis under standard conditions

	LeRoy et al.	Electrochemistry Handbook	JANAF
$\Delta H^\circ_{H_2O}$ (kJ/mol)	285.840	285.830	285.830
$\Delta G^\circ_{H_2O}$ (kJ/mol)	237.22	237.178	237.174

Table 4
Enthalpy and electrolysis voltages $V_{298,0.1}$, $E_{298,0.1}$ for water electrolysis under standard conditions

	LeRoy et al.	Electrochemistry Handbook	JANAF
$V_{298,0.1}$ (V)	1.481	1.481	1.481
$E_{298,0.1}$ (V)	1.229	1.229	1.229

Table 5
Temperature change of enthalpy voltage $V_{T,0.1}$

T (K)	LeRoy et al. (V)	Electrochemistry Handbook (V)
298	1.4813	1.4812
320	1.4779	1.4776
373	1.469	1.469
523	1.4417	1.441

3.2. Temperature change of ΔH and ΔG

The temperature change of enthalpy voltage $V_{t,1}$ is shown in Table 5 and Fig. 2, and the change in electrolysis voltage $E_{t,1}$ is shown in Table 6 and Fig. 3. JANAF is omitted here since it closely agrees with the Electrochemistry Handbook. When the values by LeRoy et al. are compared with those by the Electrochemistry Handbook, both agree closely, and it is clear that both $V_{t,1}$ and $E_{t,1}$ fall with a rise in temperature.

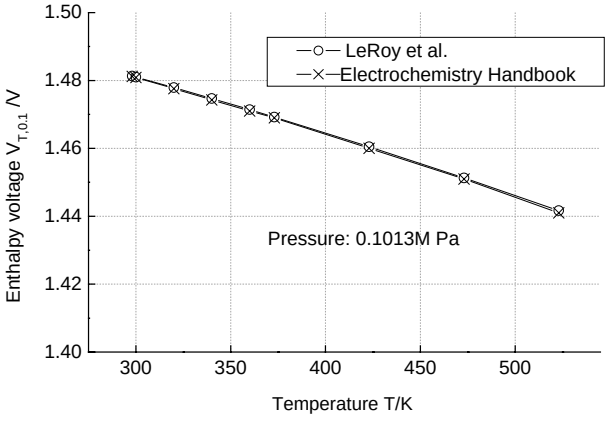

Fig. 2. Temperature change of enthalpy voltage $V_{T,0.1}$.

Table 6
Temperature change of electrolysis voltage $E_{T,0.1}$

T (K)	LeRoy et al. (V)	Electrochemistry Handbook (V)
298	1.229	1.229
320	1.211	1.211
373	1.167	1.167
523	1.051	1.050

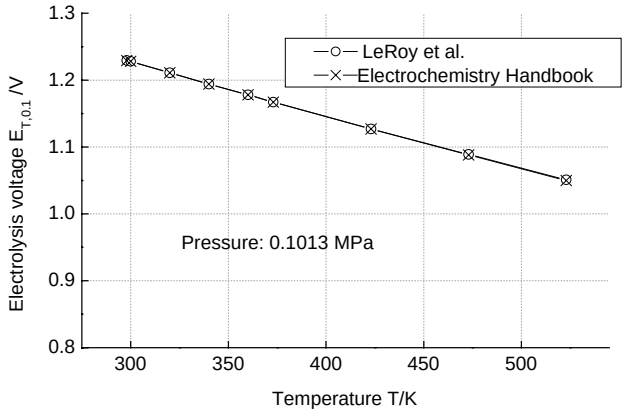

Fig. 3. Temperature change of electrolysis voltage $E_{T,0.1}$.

3.3. Pressure change of ΔH and ΔG

When determining the pressure change of ΔH and ΔG by LeRoy et al. or our data, the discrepancy is only due to the difference in the publishing year of referred steam tables. To determine the degree of error, the pressure change of $V_{25,p}$ at 25 °C is shown in Table 7 and Fig. 4. The pressure change of $E_{25,p}$ obtained by the steam tables and Eq. (16) is shown in Table 8 and Fig. 5. Although LeRoy et al. have reported $V_{25,p}$ but have not reported $E_{25,p}$, their $E_{25,p}$ is not compared in Table 8. The pressure change of $E_{25,p}$ is clearly rather large compared with $V_{25,p}$. Since the difference in the two at $V_{25,p} - V_{25,1}$ is small below approximately 0.01 mV, the pressure change of $V_{25,p}$ and $E_{25,p}$ above 100 atm can be calculated with adequate reliability. Therefore, the electrolysis power under high-pressure is predicted in a later chapter using these data.

Table 7
Change of enthalpy voltage $V_{298,p}$ by pressure

p (MPa)	LeRoy et al.		This report	
	$V_{298,p}$ (V)	$V_{298,p} - V_{298,0.1}$ (mV)	$V_{298,p}$ (V)	$V_{298,p} - V_{298,0.1}$ (mV)
0.101325	1.481	0	1.481	0
2.5	1.481	0.578	1.481	0.581
5.0	1.480	1.143	1.480	1.141
10.0	1.479	2.208	1.479	2.198

Table 8
Change of electrolysis voltage $E_{298,p}$ by pressure

p (MPa)	This report	
	$E_{298,p}$ (V)	$E_{298,p} - E_{298,0.1}$ (mV)
0.101325	1.229	0
2.5	1.290	61.61
5.0	1.304	74.83
10.0	1.317	87.92

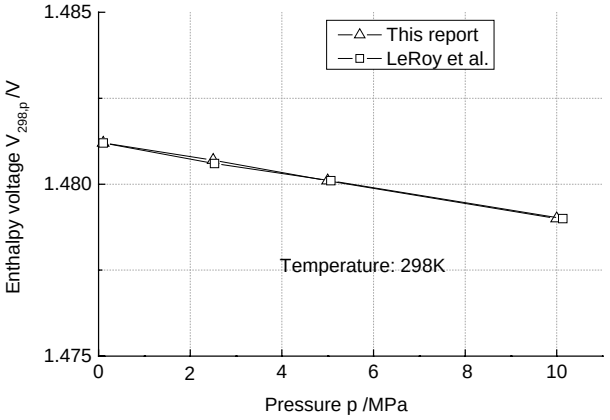

Fig. 4. Change of enthalpy voltage $V_{298,p}$ by pressure.

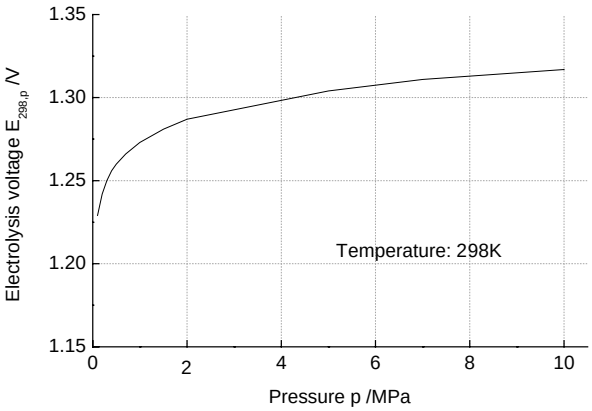

Fig. 5. Change of electrolysis voltage $E_{298,p}$ by pressure.

3.4. Pressure and temperature change of ΔH and ΔG

As the pressure change of $V_{25,p}$ and $E_{25,p}$ were confirmed to be consistent with those by LeRoy et al. up to 100 atm, we calculated the pressure change of $V_{t,p}$ above 100 atm, and this, along with the temperature change, is shown in Table 9 and Fig. 6, where the portions with no data at 250 °C indicate that liquid water is nonexistent in this range. Temperature change of $V_{t,1}$ for t (°C) and 1 atm was first calculated

Table 9
Change of enthalpy voltage $V_{T,p}$ by pressure and temperature

p (MPa)	$V_{298,p}$ (V)	$V_{373,p}$ (V)	$V_{523,p}$ (V)
0.101325	1.4812	1.4691	1.4416
10	1.4790	1.4682	1.4417
22.064	1.4768	1.4668	1.4420
40	1.4745	1.4661	1.4426
70	1.4730	1.4655	1.4443

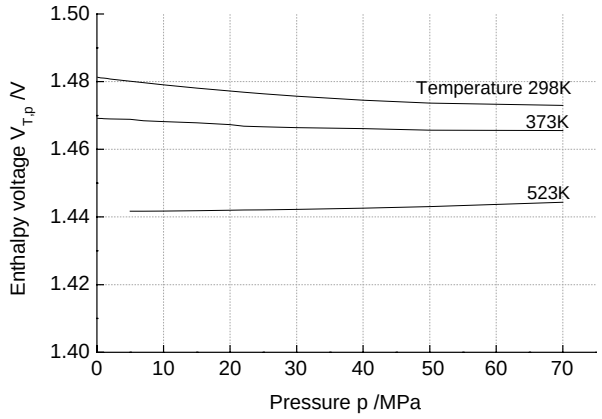

Fig. 6. Change of enthalpy voltage $V_{T,p}$ by pressure and temperature.

using Eq. (13). Then finding $H(t, p)$ of hydrogen and oxygen using Eq. (15) and $H(t, p)$ of water using the steam tables, the pressure change of $V_{t,p}$ at t (°C) was calculated. Table 9 shows that pressure has a smaller effect upon $V_{t,p}$ than temperature.

Pressure and temperature change of $E_{t,p}$ are shown in Table 10 and Fig. 7. Just as for $V_{t,p}$, the temperature change of $E_{t,1}$ for t (°C) and 1 atm was first determined by using Eq. (14). Then finding $G(t, p)$ of hydrogen and oxygen by Eq. (16) and $G(t, p)$ of water by the steam tables, the pressure change of $E_{t,p}$ at t (°C) was calculated. Pressure exerts a large effect upon $E_{t,p}$ up to approximately 100 atm, but above 100 atm voltage changes little even when pressure increases. Table 10 reveals that when 25 °C water is used for high-pressure water electrolysis, voltage increases about

Table 10
Change of electrolysis voltage $E_{T,p}$ by pressure and temperature

p (MPa)	$E_{298,p}$ (V)	$E_{373,p}$ (V)	$E_{523,p}$ (V)
0.101325	1.229	1.167	(1.051)
10	1.317	1.278	1.207
22.064	1.332	1.297	1.234
40	1.343	1.311	1.255
70	1.354	1.325	1.275

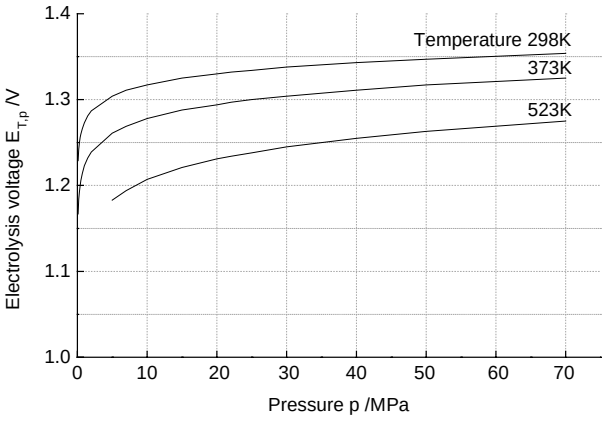

Fig. 7. Change of electrolysis voltage $E_{T,p}$ by pressure and temperature.

90 mV at 100 atm and about 110 mV at 400 atm in comparison with voltage at 1 atm. In the above, while temperature and pressure changes of $V_{t,p}$ and $E_{t,p}$ were calculated from 25 °C at 1 atm up to t (°C) followed by changes up to p (atm), the results were the same even when the changes up to p (atm) were first calculated followed by the changes up to t (°C).

4. Electrolysis power considering gas compressor and water pump power

Taking into consideration the temperature and pressure changes, we were able to measure, as mentioned above, the ideal power $W_{\mathrm{ele},t,p}$ for high-pressure water electrolysis at t (°C) and p (atm). To measure the actual production power of high-pressure hydrogen by water electrolysis, the power for the gas compressor W_{comp} and for the liquid pump W_{pump} were calculated. Essentially the realistic power for high-pressure water electrolysis should be considered including overpotential losses, but we used the ideal electrolyzing power due to the lack of overpotential data. Using the compressor and pump power, the hydrogen production power at a water flow rate of 1 mol/s was calculated as described below for high-pressure water electrolysis after water was pressurized using a high-pressure pump ($W_{\mathrm{pump}} + W_{\mathrm{ele},25,p}$), and for compression of hydrogen-gas after atmospheric water electrolysis ($W_{\mathrm{ele},25,1} + W_{\mathrm{comp}}$). First the power W_{comp} (W) required to compress electrolytic hydrogen was calculated using the following equation

$$W_{\mathrm{comp}} = \frac{\kappa}{\kappa - 1} p_1 \frac{Q_{\mathrm{N}}}{3600} \frac{T_1}{273.15} z \left\{ \left(\frac{p_2}{p_1} \right)^{\kappa - 1/\kappa} - 1 \right\} \quad (20)$$

where Q_{N} represents the intake-gas volume flow rate (N m^3/h), p_2 the discharge pressure (Pa), κ the ratio of specific heat (−), and z the compressibility factor (−). In this calculation, hydrogen of $T = 298.15$ K, $p_1 = 0.101325$ MPa, $Q_{\mathrm{N}} = 80.7$ m^3/h (corresponding to a water flow rate of 1 mol/s), $\kappa = 1.4$, and $z = 1$ was compressed by a four-stage compressor with an adiabatic efficiency assumed parametrically to be 25, 50, and 75%. The recent test data of four-stage hydrogen compressor for 40 MPa and 30 N m^3/h showed about 50% adiabatic efficiency. Next, water pump power W_{pump} (W) was calculated using the following equation

$$W_{\mathrm{pump}} = \rho g q h \quad (21)$$

where h represents the water head (m), q the water flow rate (m^3/s), ρ the water density (kg/m^3), and g the gravitational acceleration (m/s^2). Pump power was estimated also at efficiencies of 25, 50, and 75%.

Table 11 and Fig. 8 show pressure changes for $W_{\mathrm{pump}} + W_{\mathrm{ele},25,p}$ and $W_{\mathrm{ele},25,1} + W_{\mathrm{comp}}$. The numbers in parenthesis on the chart represent water pump power, and those in brackets represent hydrogen-gas compressor power. At 50%

Table 11
Change of hydrogen production power by pressure

p (MPa)	$W_{\text{pump}} + W_{\text{ele},298,p}$ (kW)	$W_{\text{ele},298,0.1} + W_{\text{comp}}$ (kW)
0.101325	237.2	237.2
10	254.5 (0.36)	264.2 [27.0]
22.064	257.8 (0.80)	269.9 [32.6]
40	260.6 (1.45)	274.3 [37.1]
70	263.8 (2.53)	278.7 [41.5]

Values in ( ) represent water pump power at $\eta = 50\%$; and in [ ], hydrogen compressor power at $\eta = 50\%$.

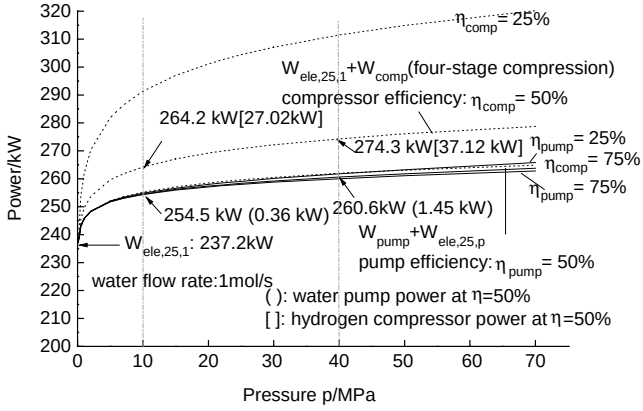

Fig. 8. Change of hydrogen production power by pressure.

efficiency, the power for high-pressure water electrolysis ($W_{\text{pump}} + W_{\text{ele},25,p}$) was about 4% and about 5% less than the power for atmospheric water electrolysis ($W_{\text{ele},25,1} + W_{\text{comp}}$), at 100 and 400 atm, respectively.

5. Conclusion

Based on the research by LeRoy et al., we have estimated temperature changes up to 250 °C and pressure changes up to 70 MPa for ideal hydrogen production power (enthalpy changes and Gibbs energy changes) of water electrolysis using polymer electrolyte membranes. Water electrolysis voltage at high-pressure decreases as temperature rises, and while it increases as pressure increases, the increase is found to be small at pressure above 20 MPa. Also, water electrolysis power is estimated for both cases of high-pressure water electrolysis after pressurizing the water ($W_{\text{pump}} + W_{\text{ele},25,p}$), and of hydrogen-gas compression after atmospheric water electrolysis ($W_{\text{ele},25,1} + W_{\text{comp}}$), examining the relative merits of highly pressurizing liquid water and hydrogen-gas. When water pump and hydrogen-gas compressor efficiencies are assumed to be 50%, it is found that hydrogen can be produced with about 5% less power using high-pressure water electrolysis than that required using atmospheric water electrolysis.

Acknowledgements

Part of this study has been carried out under the Engineering Advancement Association of Japan's WE-NET Task 8, Development of Hydrogen Production Technology, a project sponsored by NEDO, for which we wish to express our sincere appreciation.

References

[1] M. Yamaguchi, Energy Resour. 21 (2000) 38 (in Japanese).
[2] K. Onda, T. Murakami, T. Hikosaka, M. Kobayashi, R. Notu, K. Ito, J. Electrochem. Soc. 149 (2002) A1069.
[3] R.L. LeRoy, C.T. Bowen, D.J. LeRoy, J. Electrochem. Soc. 127 (1980) 1954.
[4] K. Hashizaki, Electrochemistry 71 (2003) 282 (in Japanese).
[5] A. Fujishima, Electrochemistry Handbook, fifth ed., Electrochemical Society of Japan, Maruzen, Tokyo, 2000, p. 27 (in Japanese).
[6] K. Watanabe, JSME Steam Tables, fifth ed., Japan Society of Mechanical Engineers, Maruzen, Tokyo, 1999, p. 49 (in Japanese).
[7] M.W. Chase, C.A. Davies, J.R. Downey Jr., D.J. Frurip, R.A. McDonald, A.N. Syverud, J. Phys. Chem. Ref. 14 (Suppl. 1) (1985) 1275.